Synthesis of Polypyrrole/MoO_3 Hybrid Thin Films and Their Volatile Organic Compound Gas-Sensing Properties

Kouta Hosono, Ichiro Matsubara,* Norimitsu Murayama, Shin Woosuck, and Noriya Izu

National Institute of Advanced Industrial Science & Technology, Shimo-Shidami, Moriyama-ku, Nagoya 463-8560, Japan

Received May 10, 2004. Revised Manuscript Received October 25, 2004

Thin films of the intercalated organic−inorganic hybrids $(PPy)_xMoO_3$ (PPy: polypyrrole) have been prepared by an ex-situ intercalation process. The host MoO_3 films were first deposited on $LaAlO_3$ (LAO) single-crystal substrates by using a CVD method followed by the intercalation of PPy into the MoO_3 films. The preparation of highly *b*-axis oriented MoO_3 films is crucial to prepare the $(PPy)_xMoO_3$ films. The $(PPy)_xMoO_3$ thin film shows a semiconducting-like transport with an activation energy of 0.21 eV. The $(PPy)_xMoO_3$ thin films show a distinct response to VOCs by increasing their electrical resistivity and exhibit higher sensitivities to polar analytes such as formaldehyde and acetaldehyde, whereas it showed almost no response to toluene and benzene.

Introduction

Intercalation is possible only when the binding between the layers of the host materials is very weak. This technique has been applied to develop nanohybrid materials that represent a new class of materials with the desirable physical and chemical characteristics of both organic and inorganic components within a single molecular-scale composite.[1−3] In recent years, the intercalated organic−inorganic materials have attracted much attention because of their unique microstructure and potentially useful properties involving chemical sensors, field-effect transistors, light emitters, and batteries.[4−8]

One of the most interesting properties of the orthorhombic MoO_3 is its intercalation ability. The structure of MoO_3 consists of vertex-sharing chains of distorted MoO_6 octahedra, which share edges with two similar chains to form layers. The two-dimensionally bonded double-octahedra oxide sheets are stacked in a layered arrangement and are held together by weak van der Waals forces (Figure 1). Many organic components can be intercalated into the interlayers.[9−14] We have synthesized polypyrrole (PPy) intercalated molybdenum oxide (MoO_3) hybrid materials, $(PPy)_xMoO_3$ (Figure 1), using a concomitant ion exchange reaction in a powder form.[15] The pressed pellets of the $(PPy)_xMoO_3$ powder show a distinct response to volatile organic compounds (VOCs) by increasing their electrical resistivity, which could be induced by the incorporation of VOC molecules into the interlayers of $(PPy)_xMoO_3$.[15] The $(PPy)_xMoO_3$ pellets exhibit higher sensitivities to polar analytes such as formaldehyde and acetaldehyde, whereas they show almost no response to toluene and benzene.[15] The $(PPy)_xMoO_3$ hybrids are, therefore, potential sensing materials for the selective detection of VOCs.

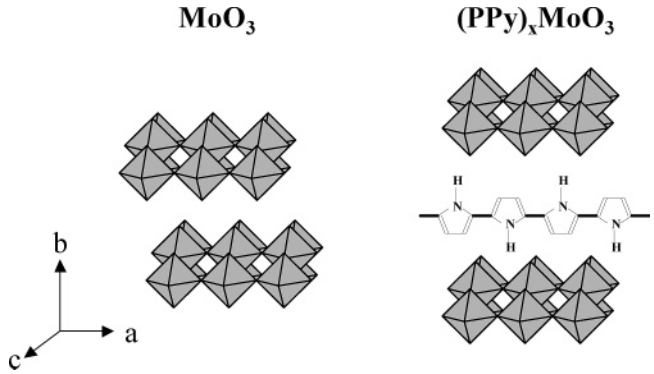

Figure 1. Schematic illustrations of the MoO_3 and $(PPy)_xMoO_3$ structures.

From the viewpoint of sensor applications of $(PPy)_xMoO_3$, it is necessary to fabricate thin film devices. Because the vapor pressure and decomposition temperature of the organic and inorganic individual compound are too different, the intercalative organic−inorganic hybrid thin films cannot be prepared by the standard techniques such as sputtering, laser ablation, coevaporation, and chemical vapor deposition (CVD). The growth of intercalative organic−inorganic hybrid

* Corresponding author. E-mail: matsubara-i@aist.go.jp.

(1) Schubert, U.; Husing, N.; Lorenz, A. *Chem. Mater.* **1995**, *7*, 2010.
(2) Sanchez, C.; Ribot, F. *New J. Chem.* **1994**, *18*, 1007.
(3) Ogawa, M.; Kuroda, K. *Chem. Rev.* **1995**, *95*, 399.
(4) Guizard, C.; Bac, A.; Barboiu, M.; Hovnanian, N. *Sep. Purif. Methods* **2001**, *25*, 167.
(5) Walcarius, A. *Chem. Mater.* **2001**, *13*, 3351.
(6) Kagan, C. R.; Mitzi, D. B.; Dimitrakopoulos, C. D. *Science* **1999**, *286*, 945.
(7) Sheeney-Haj-Ichia, L.; Wasserman, J.; Willner, I. *Adv. Mater.* **2002**, *14*, 1323.
(8) Tsure, K.; Hayakawa, S.; Ohtsuki, C.; Osaka, A. *J. Sol.-Gel Sci. Technol.* **1998**, *13*, 237.
(9) Kerr, T. A.; Wu, H.; Nazar, L. F. *Chem. Mater.* **1996**, *8*, 2005.
(10) Nazar, L. F.; Zhang, Z.; Zinkweg, D. J. *J. Am. Chem. Soc.* **1992**, *114*, 6239.
(11) Goward, G. R.; Kerr, T. A.; Power, W. P.; Nazar, L. F. *Adv. Mater.* **1998**, *10*, 449.
(12) Kerr, T. A.; Leroux, F.; Nazar, L. F. *Chem. Mater.* **1998**, *10*, 2588.
(13) Sukpirom, N.; Oriakhi, C. O.; Lerner, M. M. *Mater. Res. Bull.* **2000**, *35*, 325.
(14) Shao, K.; Ma, Y.; Cao, Y.; Chen, Z.; Ji, X.; Yao, J. *Chem. Mater.* **2001**, *13*, 250.
(15) Matsubara, I.; Murayama, N.; Shin, W.; Izu, N.; Hosono, K. *Bull. Chem. Soc. Jpn.* **2004**, *77*, 1231.

10.1021/cm0492641 CCC: $30.25
Published on Web 12/30/2004

thin films has been achieved by several alternative methods. The most widely used technique is the delamination/reassembling process, in which the organic and inorganic components are piled up from a colloidal state onto a substrate.[16−21] The thin films prepared by this method, however, have the problems of adhesion with the substrate, and the films are easily peeled off. Solution-based or evaporative thin-film techniques have been reported to prepare halide-based organic−inorganic perovskites.[22,23] Although high-quality films have been obtained, these techniques can be adopted only to halide-based perovskites and related hybrid materials. In this paper, we have prepared $(PPy)_xMoO_3$ thin films by an ex-situ intercalation process. The host MoO_3 films are first deposited on $LaAlO_3$ (LAO) single-crystal substrates by using a CVD method followed by the intercalation of PPy into the MoO_3 films. Here, we report details of the preparation method and the VOC gas-sensing properties of the $(PPy)_xMoO_3$ thin films.

Experimental Section

Chemical Vapor-Deposited MoO_3 Films. The growth of MoO_3 thin films was carried out by CVD on $LaAlO_3$ (100) and MgO (100) single-crystal substrates. The pyrolysis process of molybdenum hexacarbonyl ($Mo(CO)_6$) proceeded in an oxygen ambient at 7 Torr. The $Mo(CO)_6$ powder (50−100 mg) was placed in a glass boat and held at room temperature. Oxygen flow carried the $Mo(CO)_6$ vapors to the substrate which was heated at 420−540 °C. The oxygen flow rate was 100 mL/min, and the deposition time was varied from 15 to 90 min. Because of the high volatility of $Mo(CO)_6$, it is sublimed under vacuum, 7 Torr, even at room temperature. The detailed procedure was as follows: (i) the substrate was set on a holder, (ii) the substrate was heated at 420−540 °C, (iii) evacuation was initiated, (iv) the chamber atmosphere was returned to atmospheric pressure, and then (v) the substrate was cooled to room temperature. The deposition time was defined as the duration between the initiation and termination of the evacuation.

Intercalation Reactions with MoO_3 Films. The intercalation of PPy was carried out via a two-step process.[9] First, hydrated sodium ions were inserted into the MoO_3 layers ($[Na(H_2O)_5]_yMoO_3$), and then PPy was intercalated by ion exchange. The intercalation of hydrated sodium ions was carried out following the literature method.[24] Ar gas was bubbled through 25 mL of distilled water for 10 min. A mixture of $Na_2S_2O_4$ (0.2 g, 1.1 mmol) and $Na_2MoO_4 \cdot 2H_2O$ (6 g, 24.8 mmol) was dissolved in the distilled water, and this solution was stirred for 50 s under the bubbling of Ar gas. The MoO_3 thin films were immersed into the solution for 10 s under the bubbling of Ar gas. After the films were taken out from the solution, they were washed with distilled water and dried at 125 °C for 30 min in air to give $[Na(H_2O)_5]_yMoO_3$ films. An excess amount of pyrrole (2.0 mL, 28.9 mmol) was added to 25 mL of distilled water, and the mixture was treated with a supersonic homogenizer for 3 min. An oxidizing agent, $FeCl_3$ (0.086 g, 0.51 mmol), was added to the mixture and stirred for 10 min. The $[Na(H_2O)_2]_yMoO_3$ films were immersed into the mixture for 5 min. After the reaction, 20 mL of ethanol was added, and the reaction mixture was stirred for another 2 min. After the $(PPy)_xMoO_3$ thin films were taken out from the solution, they were washed with distilled water and ethanol, and then dried at 125 °C for 60 min in air. The intercalation reaction of PPy was carried out in air.

Instrumentation. Room-temperature X-ray diffraction (XRD) patterns were collected on a Rigaku RINT2100V/PC instrument, with a graphite monochromator to produce a Cu Kα beam, at 40 kV and 40 mA. A four-circle diffractometer was used to measure the X-ray α and β scans and to collect the pole figure. Scanning electron microscopic (SEM) observation was performed using a JEOL JSM-6355FM microscope. The films were mounted on a holder with silver paste.

Gas-sensing properties of the $(PPy)_xMoO_3$ thin films to VOCs, formaldehyde (HCHO), acetaldehyde (CH_3CHO), chloroform ($CHCl_3$), methanol (CH_3OH), ethanol (C_2H_5OH), acetone ($(CH_3)_2CO$), toluene ($CH_3C_6H_5$), and benzene (C_6H_6) balanced with air, were measured in a chamber which had a capacity of about 24 L. The measurements were carried out at room temperature. A ceramic heater and fan were set in the chamber. The heater was used to vaporize the reagents, and the fan was used to make a homogeneous test gas atmosphere. Each of the liquid VOCs was driven in the chamber using a microsyringe to realize a selected VOC gas concentration. A Au comb-type electrode was deposited by sputtering onto the $(PPy)_xMoO_3$ thin films. A couple of gold wires were connected to the electrodes using silver paste, and the resistance signal was measured directly through these wires. The sensitivity was defined as the ratio R_g/R_a, in which R_g and R_a were the electrical resistances in the explosive gas to be detected and air, respectively. Gas-sensing properties were also measured for 100 ppm HCHO balanced with air at room temperature in a flow-type apparatus. The temperature dependence of resistivity was measured under a direct current of 1 μA by the standard four-probe method.

Results and Discussion

We have developed an ex-situ intercalation process for preparing $(PPy)_xMoO_3$ thin films. By the chemical intercalation of PPy into MoO_3 films, single-phase organic−inorganic $(PPy)_xMoO_3$ thin films were formed. During the intercalation reaction, the interlayer distance of the MoO_3 sheets expands in the crystallographic *b*-axis direction of the orthorhombic MoO_3 structure by about 50%. When the host MoO_3 films have a random orientation, the films could be peeled off due to the strain generated by the interlayer expansion. In the case of highly *b*-axis oriented MoO_3 films, because the strain is generated only in the out-of-plane direction, the peeling problem could be avoided. Highly *b*-axis oriented MoO_3 films are, therefore, necessary to prepare $(PPy)_xMoO_3$ thin films in this ex-situ intercalation process.

MoO_3 thin films have been prepared by various techniques such as CVD,[25,26] sputtering,[27] flash and thermal deposition,[28]

(16) Liu, Z. H.; Yang, X. J.; Makita, Y.; Ooi, K. *Chem. Mater.* **2002**, *14*, 4800.
(17) Wang, L.; Omomo, Y.; Sakai, N.; Fukuda, K.; Nakai, I.; Ebina, Y.; Takada, K.; Watanabe, M.; Sakai, T. *Chem. Mater.* **2003**, *15*, 2873.
(18) Lakshmi, B. B.; Dorhout, P. K.; Martin, C. R. *Chem. Mater.* **1997**, *9*, 857.
(19) Choy, J. H.; Paek, S. M.; Oh, J. M.; Jang, E. S. *Curr. Appl. Phys.* **2002**, *2*, 489.
(20) Sukpirom, N.; Lerner, M. M. *Mater. Sci. Eng., A* **2003**, *354*, 180.
(21) Malzbender, T.; de With, G. *Thin Solid Films* **2001**, *386*, 68.
(22) Mitizi, D. B. Synthesis, Structure, and Properites of Organic−Inorganic Perovskites and Related Materials. *Progress in Inorganic Chemistry*; John Wiley & Sons: New York, 1999; Vol. 48.
(23) Mitzi, D. B.; Prikas, M. T.; Chondroudis, K. *Chem. Mater.* **1999**, *11*, 542.
(24) Thomas, D. M.; McCarron, E. M. *Mater. Res. Bull.* **1986**, *21*, 945.
(25) Ivanova, T.; Szekeres, A.; Gartner, M.; Gogova, D.; Gesheva, K. A. *Electrochim. Acta* **2001**, *46*, 2215.
(26) Ivanova, T.; Surtchev, M.; Gesheva, K. *Mater. Lett.* **2002**, *53*, 250.
(27) Scarminio, J.; Lourenco, A.; Gorenstein, A. *Thin Solid Films* **1997**, *302*, 66.

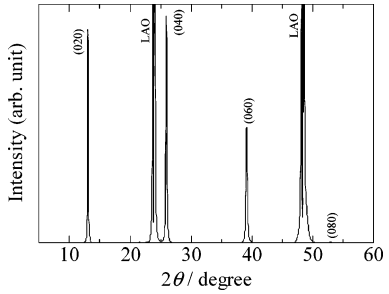

Figure 2. X-ray diffraction pattern of a MoO_3 thin film on a $LaAlO_3$ substrate.

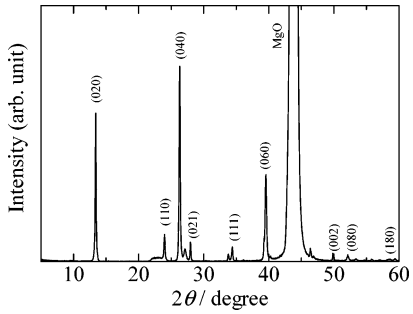

Figure 3. X-ray diffraction pattern of a MoO_3 thin film on a MgO substrate.

electrodeposition,[29] and hot-filament deposition.[30] Here, we adopted a CVD technique using a solid molybdenum source, $Mo(CO)_6$.[26] As a high vacuum environment is not necessary to deposit the films by this method, the orthorhombic MoO_3 phase is formed in the as-grown films without postannealing. Another advantageous point is a higher deposition rate to form films of substantial thickness.

Figure 2 shows the XRD pattern of a MoO_3 film deposited on LAO at 500 °C. The XRD pattern exhibits the dominant *b*-axis orientation. The interlayer spacing of MoO_3 is equal to 0.69 nm, which is consistent with the reported value.[31] No diffraction peaks due to impurity phases were observed. Figure 3 shows the XRD pattern of a MoO_3 film deposited on MgO at 500 °C. In addition to (0*k*0) peaks, many other diffraction peaks are observed, indicating that the MoO_3 thin film on MgO has a poor *b*-axis orientation as compared to that on LAO. The *a*- and *c*-axis lengths of the orthorhombic MoO_3 have been reported to be 0.3963 and 0.3696 nm, respectively.[31] The in-plane average length of the *a*- and *c*-axis is 0.3830 nm. The *a*-axis lengths of LAO and MgO are 0.3790 and 0.4216 nm, respectively. The lattice mismatch between MoO_3 and the substrate is calculated to be 1.03% and 9.97% for LAO and MgO, respectively. The poor *b*-axis orientation observed for the MgO substrate is due to the large lattice mismatch. The choice of an appropriate substrate is crucial to obtain highly *b*-axis oriented MoO_3 thin films.

The MoO_3 film on MgO consists of platelike grains with the size of 500−900 nm in diameter as shown in Figure 4a. The well-developed plane of each grain is not completely parallel to the substrate surface, indicating poor *b*-axis orientation. On the other hand, the SEM image of a MoO_3 film on LAO (Figure 4b) shows that flat and smooth planes of MoO_3 grains are distributed over the film.

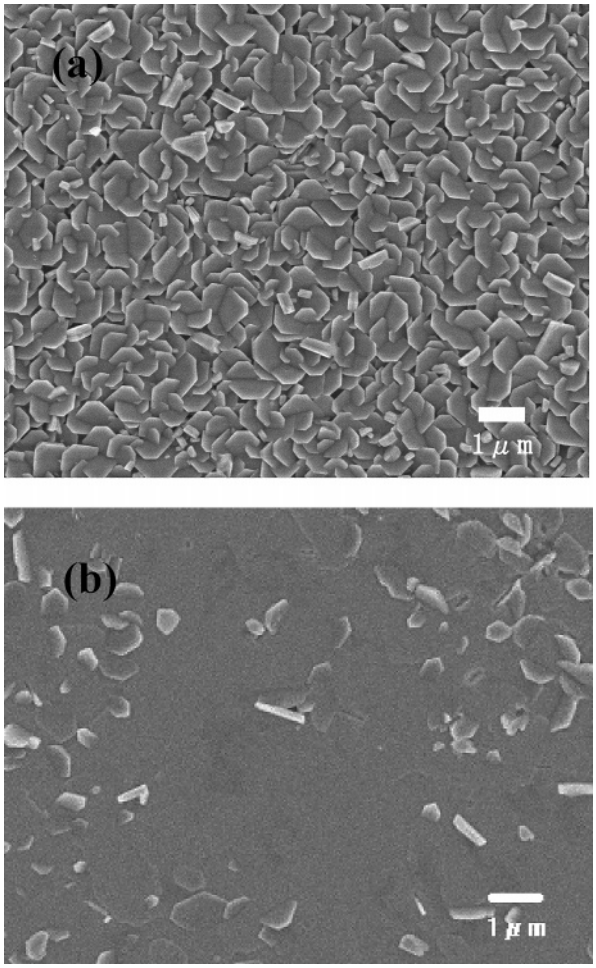

Figure 4. Scanning electron micrographs of MoO_3 thin films (a) on MgO and (b) on $LaAlO_3$ substrates.

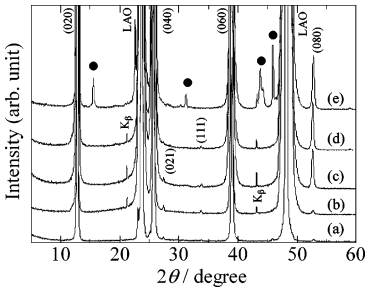

Figure 5. X-ray diffraction patterns of MoO_3 thin films deposited on $LaAlO_3$ substrates at (a) 420 °C, (b) 480 °C, (c) 500 °C, (d) 520 °C, and (e) 540 °C. Impurity peaks due to Mo_4O_{11} are indicated by ●.

Figure 5 shows X-ray diffraction (XRD) patterns of MoO_3 films deposited on LAO at several different substrate temperatures, 420, 480, 500, 520, and 540 °C. In the film deposited at 540 °C (Figure 5e), there are some diffraction peaks due to an oxygen-deficient Mo_4O_{11} impurity phase.[32] On the other hand, no diffraction peaks of the Mo_4O_{11} impurity phase are observed in the MoO_3 films deposited at 420−520 °C. It is proven that highly *b*-axis oriented phase-

(28) Julien, C.; Nazri, G. A.; Guesdon, J. P.; Gorenstein, A.; Khelfa, A.; Hussain, O. M. *Solid State Ionics* **1994**, *73*, 319.
(29) Guerfi, A.; Dao, L. H. *J. Electrochem. Soc.* **1989**, *136*, 2435.
(30) Bica de Moraes, M. A.; Trasferetti, B. C.; Rouxinol, F. P.; Landers, R.; Durrant, S. F.; Scarmínio, J.; Urbano, A. *Chem. Mater.* **2004**, *16*, 513.
(31) Wei, X. M.; Zeng, H. C. *J. Phys. Chem. B* **2003**, *107*, 2619.
(32) Guidi, V.; Boscarino, D.; Casorotto, L.; Comini, E.; Ferroni, M.; Martinelli, G.; Sberveglieri, G. *Sens. Actuators, B* **2001**, *77*, 555.

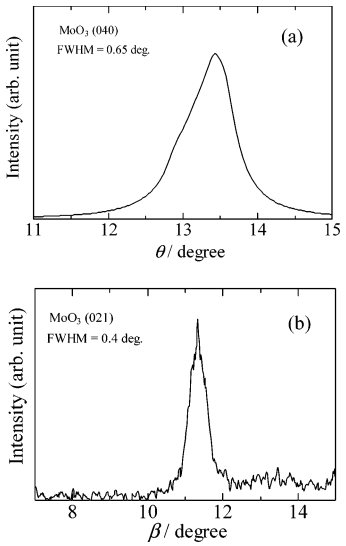

Figure 6. X-ray diffraction θ scan (a) and β scan (b) for a MoO_3 thin film on a $LaAlO_3$ (100) substrate.

pure MoO_3 films can be obtained at substrate temperatures between 420 and 520 °C without postannealing. The thickness of the MoO_3 films deposited at 420, 480, 500, 520, and 540 °C is 72, 106, 110, 350, and 422 nm, respectively. The deposition time was 90 min only for the films deposited at 420 °C, and the other films were deposited for 15 min. The growth rate increases with increasing substrate temperature. The following oxidation reaction is expected to take place at or near the heated substrate:

$$2Mo(CO)_6 + 9O_2 \rightarrow 2MoO_3 + 12CO_2$$

The film deposition rate depends on this oxidation reaction rate, and hence the deposition temperature. Even under the moderate vacuum conditions used in our CVD process, the deposition temperature of 540 °C is higher than the thermodynamically stable region of the orthorhombic MoO_3 phase.

The in-plane and out-of-plane epitaxy was evaluated by X-ray β and θ scans, respectively, for a MoO_3 film deposited on LAO at 520 °C. Figure 6a shows the θ scan (rocking curve) of the MoO_3 (040) reflection and verifies the good *b*-axis alignment with the full-width-at-half-maximum (fwhm) determined to be 0.65°. Figure 6b shows the result of a β scan obtained from the MoO_3 (021) plane. The film has a good in-plane texture with a 0.4° of fwhm, which is almost comparable to that of the (111) plane of the LAO single-crystal substrate, fwhm = 0.3°. Figure 7a shows an X-ray pole figure of the MoO_3 (021) reflection. As four double spots regularly appear, the MoO_3 films have a twin characteristic. The X-ray pole figure (Figure 7b) of the LAO (111) reflection regularly appears in four poles. As compared to Figure 7a and b, the pole of the MoO_3 (021) and LAO (111) reflection deviates by 45°, indicating a cube-on-cube epitaxy: LAO (100)//MoO_3 (100).

The intercalation reactions were carried out for the MoO_3 thin films deposited on LAO and MgO substrates. Figure 8 shows XRD patterns of the $[Na(H_2O)_2]_yMoO_3$ and $(PPy)_x$-MoO_3 thin films on LAO. The intercalation of hydrated sodium ions expands the interlayer spacing by 0.28 nm as

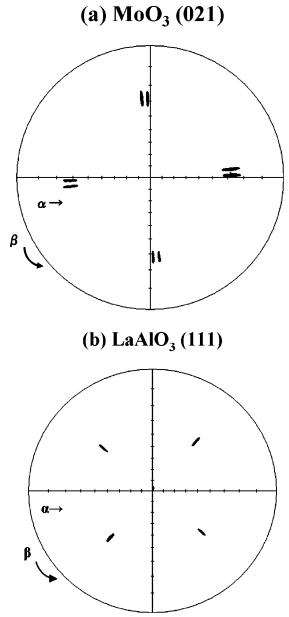

Figure 7. Pole figure plots of a MoO_3 film on $LaAlO_3$: (a) taken for MoO_3 (021), and (b) taken for $LaAlO_3$ (111).

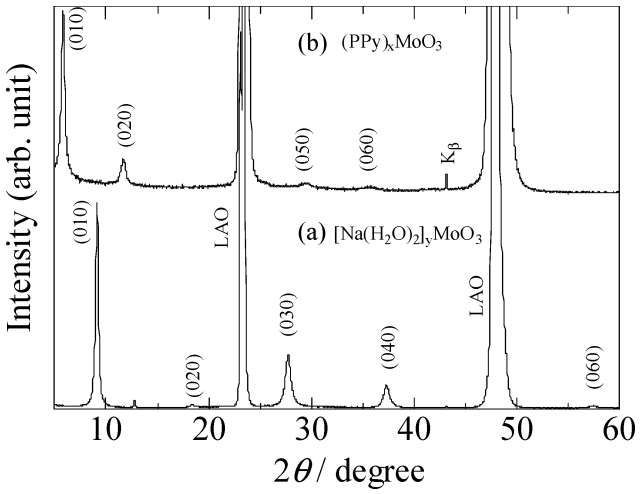

Figure 8. X-ray diffraction patterns of (a) $[Na(H_2O)_2]_yMoO_3$ and (b) $(PPy)_x$-MoO_3 thin films.

compared to MoO_3, indicating that $[Na(H_2O)_2]^+$ units are incorporated into the MoO_3 layers.[24] After the ion exchange reaction, the intercalated PPy expands the interlayer spacing of the MoO_3 lattice along the *b*-axis. The interlayer spacing of $(PPy)_xMoO_3$ is equal to 1.47 nm, corresponding to an interlayer expansion of 0.78 nm as compared to the MoO_3, sufficient to accommodate the PPy molecules. It is noted that the *b*-axis diffraction peaks overwhelmingly dominate the diffaction pattern, with six observed (0*k*0) peaks. The presence of higher order peaks indicates that the formed $(PPy)_xMoO_3$ film is well-ordered. In the XRD pattern of the $(PPy)_xMoO_3$ thin film, no MoO_3 and $[Na(H_2O)_2]_yMoO_3$ impurity phases remain, indicating that the intercalation of PPy successfully proceeds in the present process. The intercalation reaction of PPy to form the $(PPy)_xMoO_3$ thin film is completed within several minutes, which is shorter than that for the powder sample by about 1/10. For the PPy intercalation reaction of the thin films, the stoichiometry of added PPy and $[Na(H_2O)_2]_yMoO_3$ is not the same as in the case of the powder sample. As compared to the [Na-

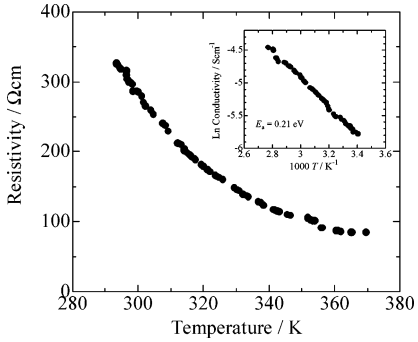

Figure 9. Temperature dependence of resistivity of the $(PPy)_xMoO_3$ thin film.

$(H_2O)_2]_yMoO_3$ powder, the amount of $[Na(H_2O)_2]_yMoO_3$ of the film used for the reaction is estimated to be about $1/10^4$. Thus, the $[Na(H_2O)_2]_yMoO_3$ thin films were reacted with a larger excess amount of PPy, which could play a role in reducing the reaction time.

The MoO_3 thin films deposited on MgO tended to peel off from the substrate during the intercalation process of the hydrated sodium ions. Because the MoO_3 films on MgO have a poor *b*-axis orientation, the interlayer expansion due to the intercalation could induce strain in the in-plane direction, which causes the film peeling. In the case of the *b*-axis oriented films, the interlayer expansion is limited to the out-of-plane direction, and no in-plane strain could be generated. Therefore, highly *b*-axis oriented MoO_3 thin films are required to obtain the $(PPy)_xMoO_3$ films.

Figure 9 shows the temperature dependence of the resistivity (ρ) for $(PPy)_xMoO_3$ thin film deposited on LAO at 500 °C. The resistivity measurements were carried out by passing a direct current parallel to the well-oriented ac-plane. The room-temperature resistivity was 285 Ω cm. A thermally activated transport ($d\rho/dT < 0$) is observed for the measured temperature range. The $(PPy)_xMoO_3$ film shows a linear relationship in the $\ln(\rho)$ versus $1/T$ plot (see Figure 9). The apparent activation energy is calculated to be 0.21 eV, which is consistent with that of the $(PPy)_xMoO_3$ pressed pellet, 0.20 eV,[15] and other polymer intercalated molybdenum oxides such as $(polyaniline)_xMoO_3$ (0.2 eV)[9] and $[poly(p\text{-}phenylenevinylene)]_xMoO_3$ (0.2 eV).[10] The activation energy does not seem to depend on the polymer species. The temperature dependence of the conductivity of conducting polymers is well described by the variable-range-hopping law, $\rho = \rho_0(T/T_0)^{1/2} \exp((T_0/T)^{1/4})$, where ρ_0 is a virtually temperature-independent material parameter and T_0 is a measure for the degree of charge carrier localization.[33] Conducting polymers do not give a linear relationship in the $\ln(\rho)$ versus $1/T$ plot. These results imply that the MoO_3 host layers play a dominant role in determining the transport properties of $(PPy)_xMoO_3$.

A scanning electron microscopy image of the surface of the $(PPy)_xMoO_3$ thin film on LAO is shown in Figure 10. Enhanced platelike grains with a size of 1−3 μm are distributed over the film. The platelike shape of the grains of the pristine MoO_3 thin film is maintained even after the intercalation of PPy. The grain size of the $(PPy)_xMoO_3$ thin film is comparable to that of the pristine MoO_3, 1−3 μm, indicating that the intercalation of PPy is topotactic, as in the case of the powder sample.[15]

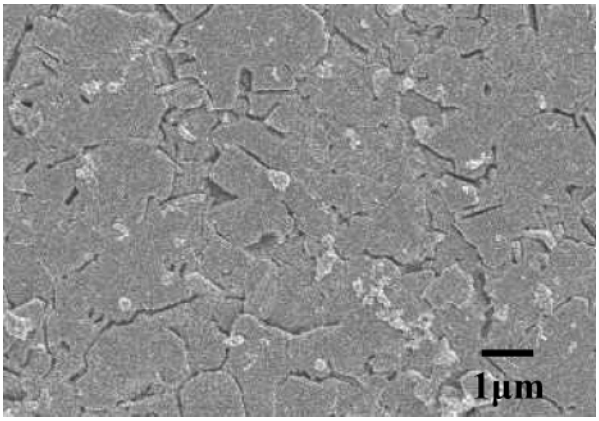

Figure 10. Scanning electron micrograph of $(PPy)_xMoO_3$ thin film on a $LaAlO_3$ substrate.

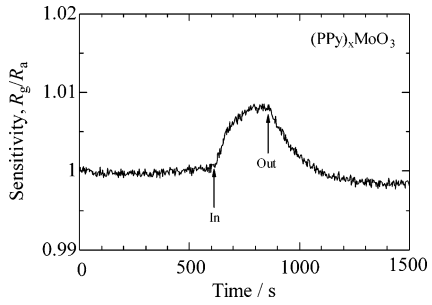

Figure 11. Room-temperature dynamic response of the $(PPy)_xMoO_3$ thin film to 100 ppm formaldehyde gas.

The gas-sensing properties of the $(PPy)_xMoO_3$ thin film to formaldehyde were evaluated. Air and a 100 ppm formaldehyde/air mixture gas were alternatively flowed into the measurement chamber at a flow rate of 100 mL/min. Figure 11 shows the response curve of the $(PPy)_xMoO_3$ thin film to formaldehyde gas at room temperature. Upon exposure to formaldehyde gas, the electrical resistance increased. When the supply of the formaldehyde gas stopped, the resistance value returned to almost the original one. The $(PPy)_xMoO_3$ thin film exhibits the distinct sensor response to formaldehyde gas by increasing its electrical resistance. The 90% response time to formaldehyde is about 140 s, which is comparable to that of the polypyrrole-poly(vinyl alcohol) composite films prepared by electrochemical polymerization.[34] Figure 12 shows the relationship between the sensitivity, (R_g/R_a), of the $(PPy)_xMoO_3$ thin film and formaldehyde gas concentration (250−2600 ppm) at room temperature. The sensitivity values are determined after the resistance change is saturated. The $(PPy)_xMoO_3$ thin film exhibits an almost linear relationship in the measured gas concentration range.

We also measured the sensitivity of the $(PPy)_xMoO_3$ thin film to other VOCs, acetaldehyde, methanol, ethanol, chloroform, acetone, toluene, and benzene, with the concentration of 1000 ppm at room temperature (Figure 13).

(33) Kanazawa, K. K.; Diaz, A. F.; Gill, W. D.; Grant, P. M.; Street, G. B.; Gardini, G. P. *Synth. Met.* **1980**, *1*, 329.

(34) Lin, C. W.; Hwang, B. J.; Lee, C. R. *Mater. Chem. Phys. B* **2003**, *107*, 2619.

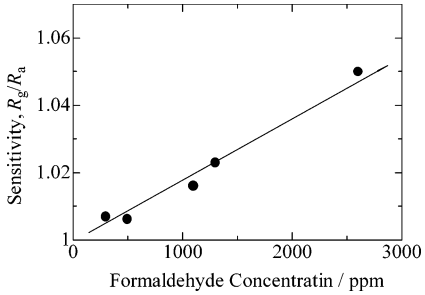

Figure 12. Relationship between the sensitivity and formaldehyde gas concentration.

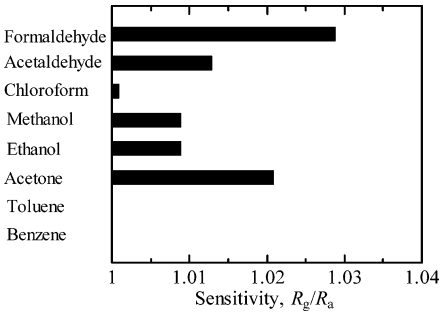

Figure 13. Magnitude of the sensitivity, R_g/R_a, of the $(PPy)_xMoO_3$ thin film at room temperature upon exposure of VOCs with a concentration of 1000 ppm.

The resistance increasing response was obtained for all of these VOCs except for benzene and toluene. The $(PPy)_xMoO_3$ thin film exhibits higher sensitivities to formaldehyde and acetone, whereas it shows almost no response to toluene and benzene. The highest sensitivity was obtained for formaldehyde. Such sensing properties obtained for the $(PPy)_xMoO_3$ thin film are consistent with that obtained for the $(PPy)_xMoO_3$ pressed pellet,[15] indicating that we have developed an effective thin film process for $(PPy)_xMoO_3$ without losing its sensing characteristics to VOCs. These $(PPy)_xMoO_3$ thin films are potential materials for sensor devices for highly selective detection of VOCs.

The response to VOCs is induced by the incorporation of analyte molecules into the interlayers of $(PPy)_xMoO_3$.[15] The insertion of analyte vapors causes two effects on the conductivity of the hybrid materials. One is the change in the interlayer distance, which could affect the degree of the electrical interaction between the PPy and MoO_3 layers, and hence the conductivity of the hybrid materials. The other is a direct electrical interaction between the analytes and $(PPy)_xMoO_3$. The charge transfer from $(PPy)_xMoO_3$ to the incorporated and adsorbed analyte molecules may reduce the concentration of the charge carriers. A detailed study on the sensing mechanism of the hybrid materials is now in progress to elucidate the likely mechanism.

Conclusion

$(PPy)_xMoO_3$ thin films were successfully prepared by an ex-situ intercalation process. The MoO_3 thin films were deposited on LAO (100) and MgO (100) substrates by a CVD process using $Mo(CO)_6$ powder as the source material. Highly *b*-axis oriented MoO_3 thin films were deposited at 420−520 °C on LAO with a small lattice mismatch against MoO_3. A semiconducting-like transport is observed for the $(PPy)_xMoO_3$ thin films; the resistivity value is 285 Ω cm at room temperature. The $(PPy)_xMoO_3$ thin films exhibit a resistance-increasing response to VOCs, as in the case of the $(PPy)_xMoO_3$ pressed pellets. The highest sensitivity was obtained for formaldehyde, whereas no response was observed for toluene and benzene. The thin film process developed for intercalative organic−inorganic hybrid, $(PPy)_xMoO_3$, makes it possible to apply this material in VOC sensor devices.

CM0492641